

Effective nonlinear optical properties of graded metal–dielectric composite films of anisotropic particles

Ji Ping Huang

*Department of Physics, The Chinese University of Hong Kong, Shatin, New Territories, Hong Kong, and
Max Planck Institute for Polymer Research, Ackermannweg 10, 55128 Mainz, Germany*

Kin Wah Yu

Department of Physics, The Chinese University of Hong Kong, Shatin, New Territories, Hong Kong

Received October 27, 2004; revised manuscript received February 8, 2005; accepted February 20, 2005

We study the effective third-order nonlinear susceptibility of a graded metal–dielectric composite film of anisotropic particles with weak nonlinearity by invoking the local field effects within the Maxwell–Garnett theory. We further numerically demonstrate that the film can serve as a novel optical material to produce a broad structure in both the linear and the nonlinear response and an enhancement in the nonlinear response.

© 2005 Optical Society of America

OCIS codes: 160.4330, 310.6860, 160.4670, 160.4760.

1. INTRODUCTION

Metal–dielectric composites have received much attention because of the potential application of their linear and nonlinear optical properties.^{1–15} Crucial elements for control of these properties are the microstructure of the composite, particle shape, and material dispersity. For anisotropically shaped metallic nanoparticles, the resonant plasmon bands split up for orientations along major and minor axes. Furthermore, in the case of a large aspect ratio, the plasmon bands may shift into the infrared, thus enabling use of metal nanostructures in telecommunication applications in this wavelength range. Compared with spherically shaped particles, anisotropically shaped metallic particles can show reduced plasmon relaxation times¹⁶ as well as enhanced nonlinear responses¹⁷ and may thus be used as building blocks in a variety of optical devices. Some techniques have been developed to fabricate rod-shaped metallic nanoparticles by lithographic means¹⁸ or anisotropic growth. Recently, it was demonstrated that mega-electron-volt (MeV) ion irradiation can also be used to modify the shape of nanoparticles.¹⁹ This ion-beam-induced anisotropic deformation effect is known to occur not only for a broad range of amorphous materials,²⁰ but also for crystalline materials including metals.¹⁵ That is, prolate spheroidal metallic particles in a dielectric host can readily be formed by irradiation of MeV ions.

The optical property of thin films^{21–25} is often different from that of the corresponding bulk material. Recently, a metal–dielectric composite (Au:BaTiO₃) film was investigated, and a large figure of merit (FOM) was observed.²⁶ In the present work, the FOM denotes the ratio of a third-order nonlinear susceptibility to an optical absorption.²⁷ If there were a larger third-order nonlinear susceptibility

or a smaller linear optical absorption under certain conditions, the corresponding FOM should be relatively larger, thus making it an attractive option. In general, graded materials^{28,29} have quite different physical properties from the homogeneous materials. In particular, graded thin films were found to show better dielectric properties than single-layer films.³⁰ However, traditional theories^{31,32} cannot be used to deal with the composites of graded particles directly. For this purpose, we put forth a first-principles approach^{33,34} and a differential effective dipole approximation.³⁵ Also, a large nonlinearity enhancement was found for a subwavelength multilayer film of titanium dioxide and conjugated polymer.¹⁰ However, the surface-plasmon resonant nonlinearity enhancement often occurs concomitantly with a strong absorption, and unfortunately this behavior causes the FOM of the resonant enhancement peak to be too small to be useful. To circumvent this problem, we shall consider a kind of graded metal–dielectric composite film, in which a dielectric (or metallic) component is introduced as anisotropically shaped particles embedded in a metallic (or dielectric) component with a compositional or shape-dependent gradation profile.

This paper is organized as follows. In Section 2 we present a theory for the graded metal–dielectric composite film of anisotropically shaped particles with weak nonlinearity, and both the effective linear dielectric constant and the third-order nonlinear susceptibility of the graded structure are derived exactly within the Maxwell–Garnett theory. In Section 3 we numerically calculate the linear optical absorption, the enhancement of the third-order optical nonlinearity, and the FOM under different conditions. We end the paper with a discussion and conclusion in Section 4.

2. FORMALISM

Let us consider a metal–dielectric composite film with a variation of volume fraction of anisotropic particles along the z axis perpendicular to the film (Fig. 1). In this case, the local constitutive relation between the displacement field $\mathbf{D}(\mathbf{r}, \omega)$ and the electric field $\mathbf{E}(\mathbf{r}, \omega)$ is given by

$$\mathbf{D}(\mathbf{r}, \omega) = \epsilon(\mathbf{r}, \omega)\mathbf{E}(\mathbf{r}, \omega) + \chi(\mathbf{r}, \omega)|\mathbf{E}(\mathbf{r}, \omega)|^2\mathbf{E}(\mathbf{r}, \omega), \quad (1)$$

where $\epsilon(\mathbf{r}, \omega)$ and $\chi(\mathbf{r}, \omega)$ are the linear dielectric constant and third-order nonlinear susceptibility of a layer inside the graded film, respectively. Here both $\epsilon(\mathbf{r}, \omega)$ and $\chi(\mathbf{r}, \omega)$ are the gradation profiles as a function of position \mathbf{r} and field frequency ω .

In the present work, the weak nonlinearity condition is assumed to be satisfied. That is, the contribution of the second term [nonlinear part $\chi(\mathbf{r}, \omega)|\mathbf{E}(\mathbf{r}, \omega)|^2$] on the right-hand side of Eq. (1) is much less than that of the first term [linear part $\epsilon(\mathbf{r}, \omega)$].¹ Next we turn to the quasi-static approximation, under which the whole graded structure can be regarded as an effective homogeneous one with an effective linear dielectric constant $\bar{\epsilon}(\omega)$ and an effective third-order nonlinear susceptibility $\bar{\chi}(\omega)$. In this connection, $\bar{\epsilon}(\omega)$ and $\bar{\chi}(\omega)$ are defined as¹

$$\mathbf{D}_0 = \bar{\epsilon}(\omega)\mathbf{E}_0 + \bar{\chi}(\omega)|\mathbf{E}_0|^2\mathbf{E}_0, \quad (2)$$

where \mathbf{D}_0 and $\mathbf{E}_0(=E_0\hat{e}_z)$ are, respectively, the volume-averaged displacement field and the electric field within the whole graded composite film.

For calculating the nonlinear optical response, we shall apply a two-step solution. In step A, we first derive the responses of a layer inside the graded film, $\bar{\epsilon}(z, \omega)$ and $\bar{\chi}(z, \omega)$. In step B, the overall responses of the graded film, $\bar{\epsilon}(\omega)$ and $\bar{\chi}(\omega)$, are derived. In the two-step solution, we note that the local field inside the spheroidal particles is uniform, and the effective nonlinear response of a layer is therefore exact within the Maxwell–Garnett theory. When we have a nonlinear host, we have to invoke the decoupling approximation.³⁶ It is worth noting that step B is exact [see Eqs. (16)–(18)]. In step A, we homogenize the composite film along the x, y plane whereas in step B we further homogenize the graded film along the z axis.

A. Responses of a Layer inside the Graded Film: $\bar{\epsilon}(z, \omega)$ and $\bar{\chi}(z, \omega)$

It is not possible to calculate $\bar{\epsilon}(z, \omega)$ exactly in terms of the compositional or shape-dependent gradation profile. Nev-

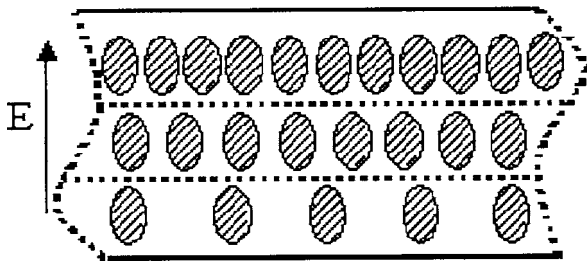


Fig. 1. Schematic graph showing the geometry of a metal–dielectric composite film with a variation of the volume fraction of anisotropic particles along the z axis perpendicular to the film. The electric field E is parallel to the gradient (z axis), thus being perpendicular to the film.

ertheless, to obtain an estimate of $\bar{\epsilon}(z, \omega)$, we can take a small volume element inside the layer at position z . Furthermore, this small volume element can be seen as a composite where the locations of the inclusion particles are random in the host medium. This, however, is a highly directional distribution since the long or short axis of prolate or oblate particles is parallel to the gradient along the z axis. Accordingly, the volume fraction of the inclusion is $p(z)$ for the dielectric or $1-p(z)$ for the metal. In this regard, the well-known Maxwell–Garnett approximation holds well to compute $\bar{\epsilon}(z, \omega)$ [as shown in Eqs. (3) and (4)]. In detail, for the dielectric particles embedded in the metallic component in a layer, $\bar{\epsilon}(z, \omega)$ can be given by the first kind of the Maxwell–Garnett approximation (MGA1)^{37–39}:

$$\frac{\bar{\epsilon}(z, \omega) - \epsilon_1(\omega)}{L_z^{(2)}\bar{\epsilon}(z, \omega) + [1 - L_z^{(2)}]\epsilon_1(\omega)} = p(z) \frac{\epsilon_2 - \epsilon_1(\omega)}{L_z^{(2)}\epsilon_2 + [1 - L_z^{(2)}]\epsilon_1(\omega)}, \quad (3)$$

where $L_z^{(2)}$ is the depolarization factor of the dielectric particles along the z axis and satisfies a sum rule $L_x^{(2)} + 2L_z^{(2)} = 1$. Here $L_x^{(2)}$ is the depolarization factor of the dielectric particles along the $x(y)$ axis; ϵ_2 [or $\epsilon_1(\omega)$] stands for the dielectric constant of the dielectric (or metallic) particles; and $p(z)$ denotes the volume fraction of the dielectric particles in each layer, which is thus a compositional gradation profile as a function of position z .

Alternatively, for the metallic particles embedded in the dielectric host, the second kind of the Maxwell–Garnett approximation (MGA2) can be used to determine $\bar{\epsilon}(z, \omega)$, such that^{37–39}

$$\frac{\bar{\epsilon}(z, \omega) - \epsilon_2}{L_z^{(1)}\bar{\epsilon}(z, \omega) + [1 - L_z^{(1)}]\epsilon_2} = [1 - p(z)] \frac{\epsilon_1(\omega) - \epsilon_2}{L_z^{(1)}\epsilon_1(\omega) + [1 - L_z^{(1)}]\epsilon_2}, \quad (4)$$

where $L_z^{(1)}$ is the depolarization factor of the metallic particles along the z axis. Similarly, there exists $L_z^{(1)} + 2L_x^{(1)} = 1$ where $L_x^{(1)}$ is the depolarization factor of the metallic particles along the $x(y)$ axis. It is worth noting that $L_z < 1/3$, $= 1/3$, and $> 1/3$ indicates the fact that the metallic (or dielectric) particles exist in the form of a prolate spheroid, sphere, and oblate spheroid, respectively. In Eqs. (3) and (4), the dielectric constant of the metal $\epsilon_1(\omega)$ is given by the known Drude expression

$$\epsilon_1(\omega) = 1 - \frac{\omega_p^2}{\omega(\omega + i\gamma)}, \quad (5)$$

where ω_p denotes the bulk plasmon frequency and γ is the collision frequency. In case of $\epsilon_1(\omega) > \epsilon_2$, the MGA1 always gives an upper bound whereas the MGA2 always gives a lower bound, and vice versa. The exact result must lie between the two bounds.⁴⁰ For both the MGA1 and the MGA2, the particles under discussion are randomly embedded but their orientations are all along the z axis (i.e., perpendicular to the film). The reason is that in experiments the prolate spheroidal metallic particles can be highly oriented along the direction of irradiated ions.¹⁵ For completeness, we shall also numerically calculate the

case of oblate spheroids in Section 3.

Then we calculate the effective nonlinear response for a layer at position z , $\bar{\chi}(z, \omega)$,¹

$$\begin{aligned} \bar{\chi}(z, \omega) \mathbf{E}(z)^4 = & [1 - p(z)] \chi_1 \langle |\mathbf{E}_1(z)|^2 \mathbf{E}_1(z)^2 \rangle \\ & + p(z) \chi_2 \langle |\mathbf{E}_2(z)|^2 \mathbf{E}_2(z)^2 \rangle, \end{aligned} \quad (6)$$

where χ_1 and χ_2 are, respectively, the (intrinsic) third-order nonlinear susceptibility of the metallic and dielectric components, $E_1(z)$ [or $E_2(z)$] represents the local electric field inside the metallic (or dielectric) component within a layer at position z , $E(z)$ denotes the volume-averaged electric field within the layer, and $\langle \dots \rangle$ stands for

the volume average of ... within the layer. To estimate $\bar{\chi}(z, \omega)$, because of the existence of a nonlinear host we have to invoke the decoupling approximation³⁶

$$\langle |\mathbf{E}_i(z)|^2 \mathbf{E}_i(z)^2 \rangle = \langle |\mathbf{E}_i(z)|^2 \rangle \langle \mathbf{E}_i(z)^2 \rangle, \quad i = 1, 2. \quad (7)$$

For the sake of consistency, the local field averages $\langle |\mathbf{E}_i(z)|^2 \rangle$ and $\langle \mathbf{E}_i(z)^2 \rangle$ should be determined by use of the Maxwell-Garnett technique.⁴¹ For the MGA1, we obtain the local field averages such that

$$\langle \mathbf{E}_2(z)^2 \rangle = \frac{[L_z^{(2)}]^{-2} \epsilon_1(\omega)^2}{([1 - p(z)] \epsilon_2 + \{[L_z^{(2)}]^{-1} - [1 - p(z)]\} \epsilon_1(\omega))^2} \mathbf{E}(z)^2, \quad (8)$$

$$\langle \mathbf{E}_1(z)^2 \rangle = \theta \left[1 - \frac{p(z) [L_z^{(2)}]^{-1} \{ [L_z^{(2)}]^{-1} \epsilon_1(\omega)^2 - [1 - p(z)] [\epsilon_2 - \epsilon_1(\omega)]^2 \}}{([1 - p(z)] \epsilon_2 + \{ [L_z^{(2)}]^{-1} - [1 - p(z)] \} \epsilon_1(\omega))^2} \right] \mathbf{E}(z)^2, \quad (9)$$

$$\langle |\mathbf{E}_2(z)|^2 \rangle = \frac{[L_z^{(2)}]^{-2} |\epsilon_1(\omega)|^2}{|[1 - p(z)] \epsilon_2 + \{ [L_z^{(2)}]^{-1} - [1 - p(z)] \} \epsilon_1(\omega)|^2} \mathbf{E}(z)^2, \quad (10)$$

$$\langle |\mathbf{E}_1(z)|^2 \rangle = \theta \left(1 - \frac{p(z) [L_z^{(2)}]^{-1} \{ [L_z^{(2)}]^{-1} |\epsilon_1(\omega)|^2 - [1 - p(z)] [\epsilon_2 - \epsilon_1(\omega)]^2 \}}{|[1 - p(z)] \epsilon_2 + \{ [L_z^{(2)}]^{-1} - [1 - p(z)] \} \epsilon_1(\omega)|^2} \right) \mathbf{E}(z)^2, \quad (11)$$

with $\theta = 1/[1 - p(z)]$. Similarly, for the MGA2, the local field averages are given by

$$\langle \mathbf{E}_1(z)^2 \rangle = \frac{[L_z^{(1)}]^{-2} \epsilon_2^2}{(p(z) \epsilon_1(\omega) + \{ [L_z^{(1)}]^{-1} - p(z) \} \epsilon_2)^2} \mathbf{E}(z)^2, \quad (12)$$

$$\langle \mathbf{E}_2(z)^2 \rangle = \theta' \left[1 - \frac{[1 - p(z)] [L_z^{(1)}]^{-1} \{ [L_z^{(1)}]^{-1} \epsilon_2^2 - p(z) [\epsilon_1(\omega) - \epsilon_2]^2 \}}{(p(z) \epsilon_1(\omega) + \{ [L_z^{(1)}]^{-1} - p(z) \} \epsilon_2)^2} \right] \mathbf{E}(z)^2, \quad (13)$$

$$\langle |\mathbf{E}_1(z)|^2 \rangle = \frac{[L_z^{(1)}]^{-2} |\epsilon_2|^2}{|p(z) \epsilon_1(\omega) + \{ [L_z^{(1)}]^{-1} - p(z) \} \epsilon_2|^2} \mathbf{E}(z)^2, \quad (14)$$

$$\langle |\mathbf{E}_2(z)|^2 \rangle = \theta' \left(1 - \frac{[1 - p(z)] [L_z^{(1)}]^{-1} \{ [L_z^{(1)}]^{-1} |\epsilon_2|^2 - p(z) |\epsilon_1(\omega) - \epsilon_2|^2 \}}{|p(z) \epsilon_1(\omega) + \{ [L_z^{(1)}]^{-1} - p(z) \} \epsilon_2|^2} \right) \mathbf{E}(z)^2, \quad (15)$$

with $\theta' = 1/p(z)$.

B. Overall Responses of the Graded Film: $\bar{\epsilon}(\omega)$ and $\bar{\chi}(\omega)$

Because of the simple graded structure (Fig. 1), we can use the equivalent capacitance of a series combination to calculate the linear response (i.e., optical absorption for the graded film) $\bar{\epsilon}(\omega)$,

$$\frac{1}{\bar{\epsilon}(\omega)} = \frac{1}{W} \int_0^W \frac{dz}{\bar{\epsilon}(z, \omega)}, \quad (16)$$

where W is the thickness of the film.

By virtue of the continuity of electric displacement, we have the relation

$$\bar{\epsilon}(z, \omega) \mathbf{E}(z) = \bar{\epsilon}(\omega) \mathbf{E}_0. \quad (17)$$

Then we take one step forward to obtain the effective third-order nonlinear susceptibility $\bar{\chi}(\omega)$ as an integral

over the graded film:

$$\bar{\chi}(\omega) = \frac{1}{W} \int_0^W dz \bar{\chi}(z, \omega) \left| \frac{\bar{\epsilon}(\omega)}{\bar{\epsilon}(z, \omega)} \right|^2 \left[\frac{\bar{\epsilon}(\omega)}{\bar{\epsilon}(z, \omega)} \right]^2. \quad (18)$$

3. NUMERICAL RESULTS

In what follows, we shall do some numerical calculations. We set both χ_1 and χ_2 to be a real and positive frequency-independent constant χ_0 so that we can emphasize the enhancement of the optical nonlinearity. Without loss of generality, the film thickness W is taken to be unity. For the model calculation, we shall use the gradation profile

$$p(z) = az^m, \quad (19)$$

where a and m are constants tuning the profile.

Figure 2 shows the results obtained from the MGA1 [Eq. (3)]. In Fig. 2 we display the optical absorption $\sim \text{Im}[\bar{\epsilon}(\omega)]$, the modulus of the effective third-order optical nonlinearity enhancement $|\bar{\chi}(\omega)|/\chi_0$, and the FOM $|\bar{\chi}(\omega)|/\{\chi_0 \text{Im}[\bar{\epsilon}(\omega)]\}$ as a function of the incident angular frequency ω for different $L_z^{(2)}$. Here $\text{Im}[\dots]$ means the imaginary part of \dots . When the layer gradation profile $p(z)=az^m$ is taken into account, a broad resonant plasmon band is observed for any $L_z^{(2)}$ of interest. In other words, the broad band is caused to appear by the effect of the positional dependence of the dielectric or metallic component. This conclusion can be made by comparing the curves in Fig. 2 with those of $n=0$ (corresponding to the case in which the effects of gradation as well as the nonspherical shape are excluded) in Fig. 7. Moreover, we find that decreasing $L_z^{(2)}$ makes the resonant bands in both optical nonlinearity and optical absorption broader. Although the enhancement of the effective third-order optical nonlinearity is often accompanied with the

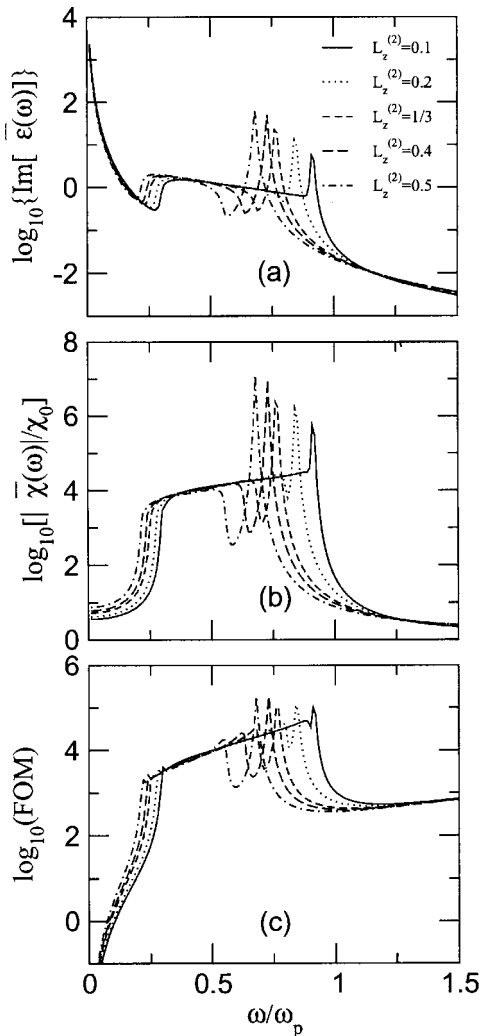


Fig. 2. Results for the MGA1 [Eq. (3)]. (a) Linear optical absorption $\text{Im}[\bar{\epsilon}(\omega)]$, (b) enhancement of the third-order optical nonlinearity $|\bar{\chi}(\omega)|/\chi_0$, and (c) $\text{FOM} \equiv |\bar{\chi}(\omega)|/\{\chi_0 \text{Im}[\bar{\epsilon}(\omega)]\}$ versus the normalized incident angular frequency ω/ω_p for a layer dielectric profile $p(z)=az^m$ for different $L_z^{(2)}$. Parameters are $a=0.8$, $m=1$, $\gamma/\omega_p=0.01$, and $\epsilon_2=(3/2)^2$.

appearance of the optical absorption, the FOM is an attractive option [see Fig. 2(c)] because of the positional dependence of the dielectric or metallic components. In particular, the particle shape can also be used to enhance the FOM significantly. It is worth noting that there is a prominent surface-plasmon resonant peak that appears at somewhat higher frequencies in addition to the surface-plasmon band at lower frequencies.

Figure 3 displays the results that were obtained from the MGA2 [Eq. (4)]. For Fig. 3, we can see that the parallel-shaped metallic particles are randomly embedded in the dielectric host in each layer. In contrast, the surface-plasmon resonant peak is found to locate at lower frequencies in addition to the surface-plasmon band that locates at higher frequencies. Also, it is shown that the broad plasmon bands in optical nonlinearity and absorption are caused by the effect of gradation, when we compare the curves in Fig. 3 with those of $n=0$ in Fig. 8. Note that the latter corresponds to the case without the effects of gradation and nonspherical shape. Decreasing $L_z^{(1)}$

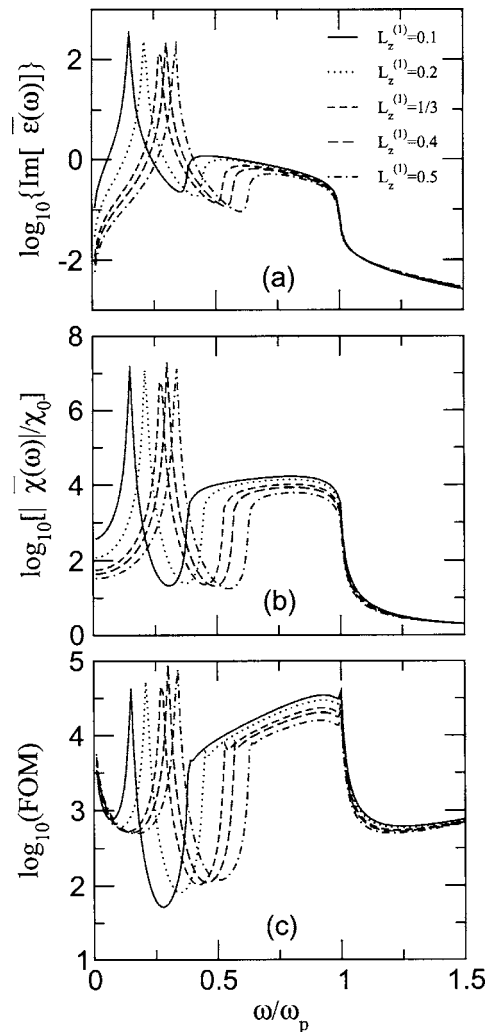


Fig. 3. Results for the MGA2 [Eq. (4)]. (a) Linear optical absorption $\text{Im}[\bar{\epsilon}(\omega)]$, (b) enhancement of the third-order optical nonlinearity $|\bar{\chi}(\omega)|/\chi_0$, and (c) $\text{FOM} \equiv |\bar{\chi}(\omega)|/\{\chi_0 \text{Im}[\bar{\epsilon}(\omega)]\}$ versus the normalized incident angular frequency ω/ω_p for a layer dielectric profile $p(z)=az^m$ for different $L_z^{(1)}$. Parameters are $a=0.8$, $m=1$, $\gamma/\omega_p=0.01$, and $\epsilon_2=(3/2)^2$.

causes the plasmon bands to be broadened. This effect makes the FOM an attractive option.

The MGA1 was applied to Fig. 4 in an attempt to show the effect of the gradation of the volume fraction of the dielectric by means of the gradation profile $p(z)=az^m$ for different a and m . In other words, we investigate a compositional gradation profile in the film, in which the dielectric particles possess a positional-dependent volume fraction. In detail, increasing a causes the resonant plasmon bands in optical nonlinearity and absorption to be broadened [see Figs. 4(a) and 4(b)]. Accordingly, in the case of gradation, the FOM can be more attractive [see Fig. 4(c)]. Similarly, Figs. 4(d) and 4(f) display the influence of m . It is apparent that the broad resonant plasmon bands in optical nonlinearity and absorption can be enhanced by increasing m [see Figs. 4(d) and 4(e)]. Finally, the FOM can become more attractive in the frequency range $0.3\omega_p < \omega < 0.7\omega_p$ as m increases [see Fig. 4(f)].

Similar to Fig. 4, Fig. 5 is plotted by the MGA2. First we discuss the effect of a . In both optical nonlinearity and absorption, the resonant plasmon bands are caused to be both enhanced and broadened by increasing a , yielding an attractive FOM in Fig. 5(c). On the other hand, the m effect on the optical nonlinearity and FOM also plays a role [see Figs. 5(e) and 5(f)]; accordingly both the optical nonlinearity and the FOM can be enhanced. In addition, as a or m varies, the plasmon resonant peaks in Fig. 5 have the same redshift (located at a lower frequency) or blueshift (located at a higher frequency) behavior as those shown in Fig. 4 where the MGA1 was used.

During ion irradiation, the ion energy can be much larger at the top of the film than that at the bottom. Therefore the particles can be prolate at the top, but they

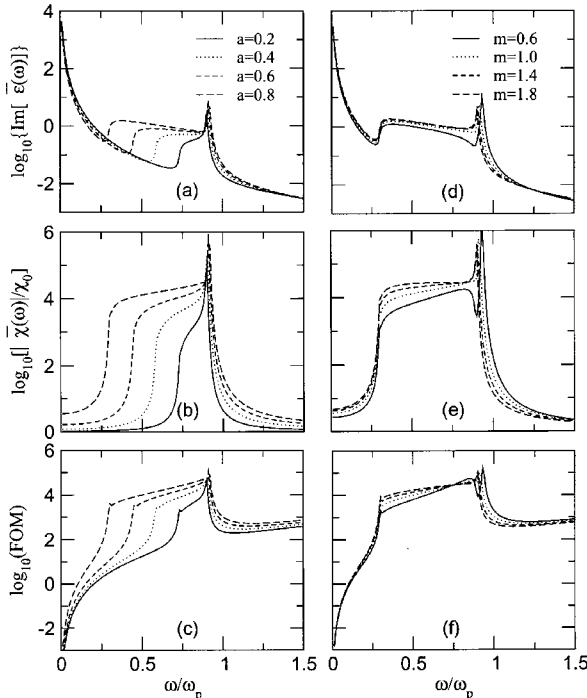


Fig. 4. Results for the MGA1 [Eq. (3)]. (a) and (d) $\text{Im}[\bar{\epsilon}(\omega)]$, (b) and (e) $|\bar{\chi}(\omega)|/\chi_0$, and (c) and (f) $\text{FOM} \equiv |\bar{\chi}(\omega)|/\{\chi_0 \text{Im}[\bar{\epsilon}(\omega)]\}$ versus ω/ω_p (a)–(c) for different a at $m=1.0$ and (d)–(f) for different m at $a=0.8$. Parameters are $L_z=0.1$, $\gamma/\omega_p=0.01$, and $\epsilon_2=(3/2)^2$.

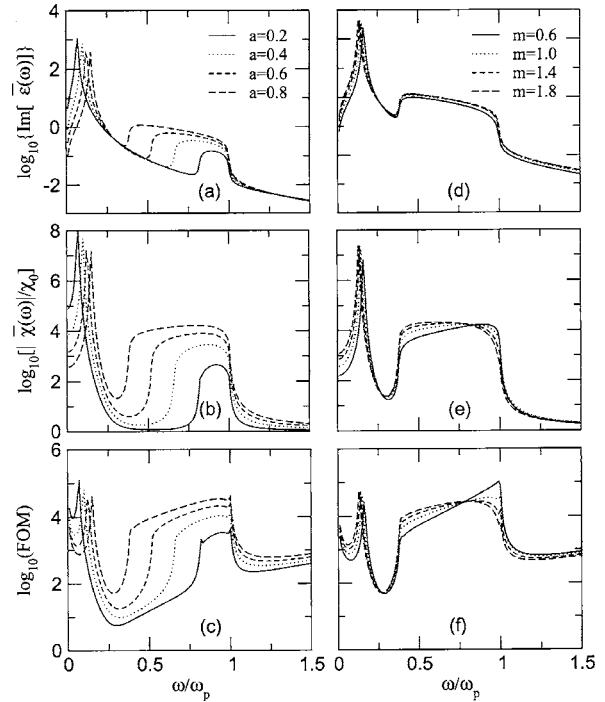


Fig. 5. Results for the MGA2 [Eq. (4)]. (a) and (d) $\text{Im}[\bar{\epsilon}(\omega)]$, (b) and (e) $|\bar{\chi}(\omega)|/\chi_0$, and (c) and (f) $\text{FOM} \equiv |\bar{\chi}(\omega)|/\{\chi_0 \text{Im}[\bar{\epsilon}(\omega)]\}$ versus ω/ω_p (a)–(c) for different a at $m=1.0$ and (d)–(f) for different m at $a=0.8$. Parameters are $L_z=0.1$, $\gamma/\omega_p=0.01$, and $\epsilon_2=(3/2)^2$.

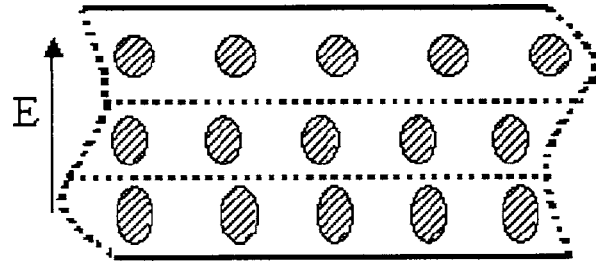


Fig. 6. Schematic graph showing the geometry of a metal-dielectric composite film with a variation of the depolarization factor of particles along the z axis perpendicular to the film. The electric field E is parallel to the gradient (z axis), thus being perpendicular to the film.

are relatively spherical at the bottom. In other words, both $L_z^{(1)}$ and $L_z^{(2)}$ can be small at the top of the film but increase to roughly $1/3$ at the bottom of the film. In this regard, we could introduce a gradation in the depolarization factor (Fig. 6) rather than in the volume fraction. Namely, in this case, $L_z(z)$ is a function of z (Fig. 6). For convenience, we keep the volume fraction constant [e.g., $p(z)=0.85$] for each layer throughout the film and take a physical profile $L_z(z)=(1/3)z^n$. In particular, as $n=0$, we have $L_z(z)=1/3$, i.e., the gradation in the depolarization factor and the nonspherical shape effect disappear. For different n , the corresponding results are shown in Figs. 7 and 8 for the MGA1 and MGA2, respectively. It is shown that the $L_z(z)$ profile does have a significant effect on the optical response, as expected. In Fig. 7(a), the plasmon peak shows a reduction as well as a blueshift as n changes from zero (without gradation) to nonzero (with gradation), and accordingly the optical nonlinearity and

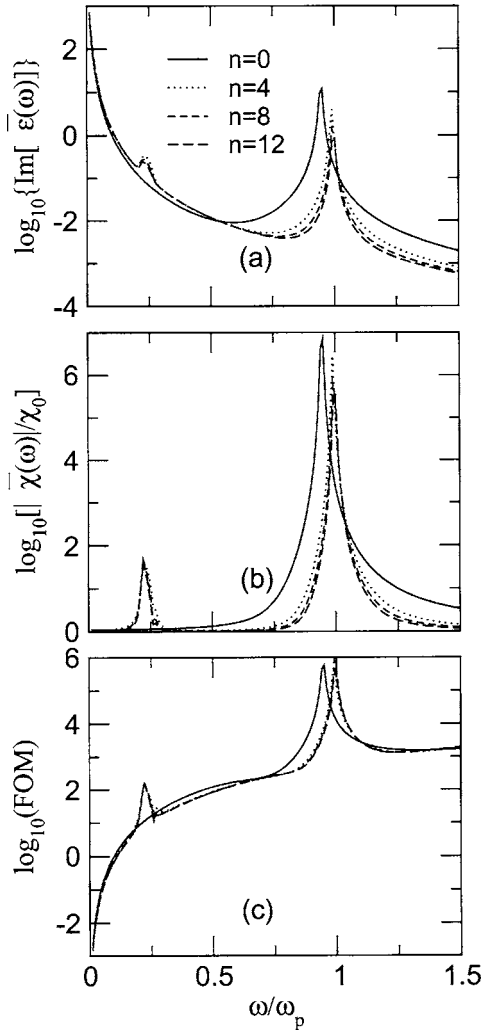


Fig. 7. Results for the MGA1 [Eq. (3)]. (a) Linear optical absorption $\text{Im}[\bar{\epsilon}(\omega)]$, (b) enhancement of the third-order optical nonlinearity $|\bar{\chi}(\omega)|/\chi_0$, and (c) $\text{FOM} \equiv |\bar{\chi}(\omega)|/\{\chi_0 \text{Im}[\bar{\epsilon}(\omega)]\}$ versus the normalized incident angular frequency ω/ω_p for the gradation profile of the depolarization factor of dielectric particles $L_z^{(2)}(z) = (1/3)z^n$ for different n . Parameters are $p(z) = 0.85$, $\gamma/\omega_p = 0.01$, and $\epsilon_2 = (3/2)^2$.

hence the FOM are reduced. The difference between the results for different nonzero n (i.e., $n = 4, 8, 12$) is not distinct (Fig. 7). Interestingly, the L_z gradation gives rise to an additional peak that appears at a lower frequency. For the MGA2 (Fig. 8), the surface-plasmon resonant bands in optical absorption and nonlinearity are clearly visible for various $L_z(z)$ profiles [see Figs. 8(a) and 8(b)]. In the presence of gradation, i.e., n becomes nonzero, the prominent plasmon absorption peak at $n = 0$ has been broadened into a plasmon band, and an additional peak is induced to appear at a lower frequency. Concomitantly, a plasmon band and a peak in optical nonlinearity also appear [Fig. 8(b)], and hence the FOM can be enhanced accordingly [see Fig. 8(c)]. On the other hand, we also find that the plasmon bands in optical absorption and nonlinearity can be further broadened (and enhanced) by adopting a wider gradation profile such as $L_z(z) = 0.5z^n$ (not shown here). For this type of profile, there are prolate particles at the top but oblate particles at the bottom of the film. It is possible

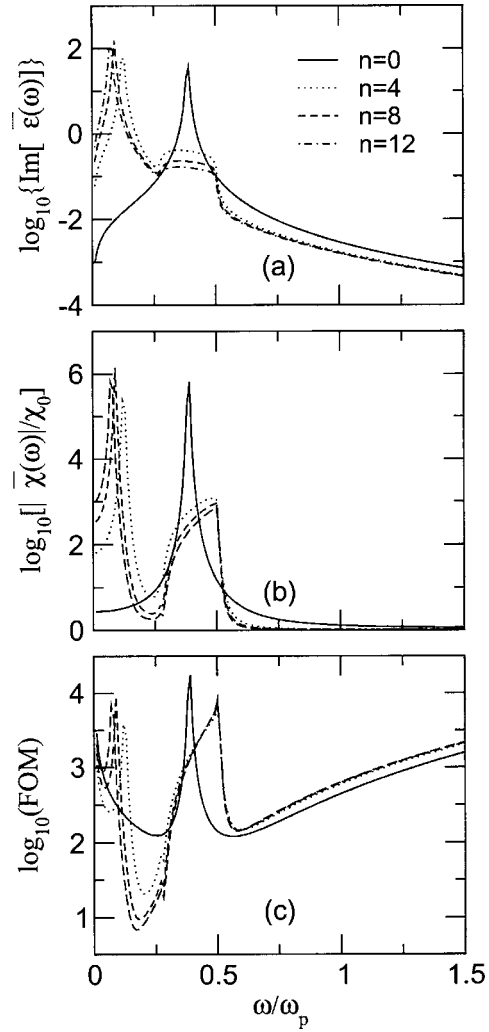


Fig. 8. Results for the MGA2 [Eq. (4)]. (a) Linear optical absorption $\text{Im}[\bar{\epsilon}(\omega)]$, (b) enhancement of the third-order optical nonlinearity $|\bar{\chi}(\omega)|/\chi_0$, and (c) $\text{FOM} \equiv |\bar{\chi}(\omega)|/\{\chi_0 \text{Im}[\bar{\epsilon}(\omega)]\}$ versus the normalized incident angular frequency ω/ω_p for the gradation profile of the depolarization factor of metallic particles $L_z^{(1)}(z) = (1/3)z^n$ for different n . Parameters are $p(z) = 0.85$, $\gamma/\omega_p = 0.01$, and $\epsilon_2 = (3/2)^2$.

to realize such oblate particles near the bottom of the film because of the reaction stress from the substance.

Finally, in Figs. 3(a), 5(a), and 8(a), there are always plasmon bands plus an absorption peak as long as the gradation profile exists. Recently, an absorption peak plus a slim plasmon absorption band were indeed observed¹⁵ in an investigation of the optical extinction spectra for ensembles of core-shell colloids with Au cores and shells embedded in an index-matching fluid. But after irradiation with 30 MeV Cu ions, a broadening of the plasmon absorption band was also observed, which was thought to attribute to the formation of Au nanorods. To account for this behavior, we believe that the particle shape and the gradation in the depolarization factor of metals and in the volume fraction of the metallic (or dielectric) component should be expected to play an important role.

To summarize, the sharp plasmon peak comes naturally from the existence of metal–dielectric interfaces. In the case of graded metallic films, there should be a broad

band only, but no sharp peak. So, for the graded metal–dielectric composite film under present consideration, both the plasmon peak and the broad plasmon band should appear as predicted above.

4. DISCUSSION AND CONCLUSION

In this paper we have studied the effective nonlinear optical response of a graded metal–dielectric composite film of anisotropic particles. On the bases of the MGA1 and MGA2 [Eqs. (3) and (4)], we derived the local electric field inside the film and hence obtained the effective linear dielectric constant [Eq. (16)] and third-order nonlinear susceptibility [Eq. (18)] of the graded composite film.

In comparison with textbook formulas, our formulas [Eqs. (3) and (4)] differ only from the z -dependent volume fraction $p(z)$, in the sense that we could discuss the gradation that is perpendicular to the film and that leads to nonlinearity enhancement. As a matter of fact, the present results do not depend crucially on the particular form of the dielectric gradation profile $p(z)$ or the depolarization factor gradation profile $L_z(z)$. The only requirement is that we must have a compositional or shape-dependent gradation to obtain a broad plasmon band for the composite film. It should be noted that the optical response of the graded structure depends on polarization of the incident light because the incident optical field can always be resolved into two polarizations. However, a large nonlinearity enhancement occurs only when the electric field is parallel to the direction of the gradient¹⁰ and the other polarization does not produce nonlinearity enhancement at all.¹⁰ The nonlinear susceptibilities of both the parallel and the perpendicular polarizations are related to the nonlinear phase shift that can be measured by using a z -scan method.¹⁰

Following Roorda *et al.*,¹⁵ one could fabricate the film under the present discussion by using MeV ion irradiation. Its third-order nonlinear susceptibility could also be measured by a degenerated four-wave-mixing method, which has been used for Au/SiO₂ composite film.²⁷ It is of interest to extend the present theory to composites in which graded spherical particles are embedded in a host medium⁴² to account for mutual interactions among graded particles.

To sum up, we have studied the effective linear dielectric constant and third-order nonlinear susceptibility of a graded metal–dielectric composite film of anisotropic particles with weak nonlinearity by invoking the local field effects exactly within the Maxwell–Garnett theory. We have numerically demonstrated that this kind of film can serve as a novel optical material to produce a broad structure in both the linear and the nonlinear response and an enhancement in the nonlinear response.

ACKNOWLEDGMENTS

We thank P. M. Hui and L. Gao for fruitful discussions and L. Dong for her collaboration. K. W. Yu thanks T. Nakayama for the invitation and hospitality during his visit to the Hokkaido University in Sapporo, Japan, where the final version of the paper was completed. This work was supported by the Research Grants Council of the Govern-

ment of the Hong Kong Special Administration Region under project number CUHK (Chinese University of Hong Kong) 403303, and by the Alexander von Humboldt Foundation in Germany (J. P. Huang).

Ji Ping Huang's e-mail address is jphuanga@alumni.cuhk.net.

REFERENCES

1. D. Stroud and P. M. Hui, "Nonlinear susceptibilities of granular matter," *Phys. Rev. B* **37**, 8719–8724 (1988).
2. G. S. Agarwal and S. Dutta Gupta, "T-matrix approach to the nonlinear susceptibilities of heterogeneous media," *Phys. Rev. A* **38**, 5678–5687 (1988).
3. X. C. Zeng, D. J. Bergman, P. M. Hui, and D. Stroud, "Effective-medium theory for weakly nonlinear composites," *Phys. Rev. B* **38**, 10970–10973 (1988).
4. D. J. Bergman, "Nonlinear behavior and $1/f$ noise near a conductivity threshold: effects of local microgeometry," *Phys. Rev. B* **39**, 4598–4609 (1989).
5. J. W. Haus, R. Inguva, and C. M. Bowden, "Effective-medium theory of nonlinear ellipsoidal composites," *Phys. Rev. A* **40**, 5729–5734 (1989).
6. B. K. P. Scaife, *Principles of Dielectrics* (Calvendon, 1989).
7. D. J. Bergman and D. Stroud, "The physical properties of macroscopically inhomogeneous media," *Solid State Phys.* **46**, 148–270 (1992).
8. J. E. Sipe and R. W. Boyd, "Nonlinear susceptibility of composite optical materials in the Maxwell Garnett model," *Phys. Rev. A* **46**, 1614–1629 (1992).
9. K. W. Yu, P. M. Hui, and D. Stroud, "Effective dielectric response of nonlinear composites," *Phys. Rev. B* **47**, 14150–14156 (1993).
10. G. L. Fischer, R. W. Boyd, R. J. Gehr, S. A. Jenekhe, J. A. Osaheni, J. E. Sipe, and L. A. Weller-Brophy, "Enhanced nonlinear optical response of composite materials," *Phys. Rev. Lett.* **74**, 1871–1874 (1995).
11. K. P. Yuen and K. W. Yu, "Optical response of a nonlinear composite film," *J. Opt. Soc. Am. B* **14**, 1387–1389 (1997).
12. V. M. Shalaev, *Nonlinear Optics of Random Media: Fractal Composites and Metal-Dielectric Films* (Springer-Verlag, 2000).
13. M. Tlidi, M. F. Hilali, and P. Mandel, "Instability of optical tetrahedral dissipative crystals," *Europhys. Lett.* **55**, 26–32 (2001).
14. P. Mulvaney, "Not all that's gold does glitter," *MRS Bull.* **26**, 1009–1014 (2001).
15. S. Roorda, T. V. Dillen, A. Polman, C. Graf, A. V. Blaaderen, and B. J. Kooi, "Aligned gold nanorods in silica made by ion irradiation of core-shell colloidal particles," *Adv. Mater. (Weinheim, Ger.)* **16**, 235–237 (2004).
16. C. Sönnichsen, T. Franzl, T. Wilk, G. V. Plessen, J. Feldmann, O. Wilson, and P. Mulvaney, "Drastic reduction of plasmon damping in gold nanorods," *Phys. Rev. Lett.* **88**, 077402 (2002).
17. K. P. Yuen, M. F. Law, K. W. Yu, and P. Sheng, "Optical nonlinearity enhancement via geometric anisotropy," *Phys. Rev. E* **56**, R1322–R1325 (1997).
18. B. M. I. V. D. Zande, L. Pages, R. A. M. Hikmet, and A. V. Blaaderen, "Optical properties of aligned rod-shaped gold particles dispersed in poly(vinyl alcohol) films," *J. Phys. Chem.* **103**, 5761–5767 (1999).
19. E. Snoeks, A. V. Blaaderen, T. V. Dillen, C. M. V. Kats, M. L. Brongersma, and A. Polman, "Colloidal ellipsoids with continuously variable shape," *Adv. Mater. (Weinheim, Ger.)* **12**, 1511–1514 (2000).
20. A. Benyagoub, S. Klaumünzer, L. Thomé, J. C. Dran, F. Garrido, and A. Dunlop, "Ion-beam induced plastic-deformation in amorphous materials investigated by maker implantation and RBS," *Nucl. Instrum. Methods Phys. Res. B* **64**, 684–686 (1992).
21. R. S. Bennink, Y.-K. Yoon, R. W. Boyd, and J. E. Sipe, "Accessing the optical nonlinearity of metals with

- metal-dielectric photonic bandgap structures," *Opt. Lett.* **24**, 1416–1418 (1999).
22. H. Grull, A. Schreyer, N. F. Berk, C. F. Majkrzak, and C. C. Han, "Composition profiling in a binary polymer blend thin film using polarized neutron reflectivity," *Europhys. Lett.* **50**, 107–112 (2000).
23. D. R. Kammler, T. O. Mason, D. L. Young, T. J. Coutts, D. Ko, K. R. Poepelmeier, and D. L. Williamson, "Comparison of thin film and bulk forms of the transparent conducting oxide solution $\text{Cd}_{1-x}\text{In}_{2-2x}\text{Sn}_x\text{O}_4$," *J. Appl. Phys.* **90**, 5979–5985 (2001).
24. J. P. Huang and K. W. Yu, "Optical nonlinearity enhancement of graded metallic films," *Appl. Phys. Lett.* **85**, 94–96 (2004).
25. J. P. Huang and K. W. Yu, "Second-harmonic generation in graded metallic films," *Opt. Lett.* **30**, 275–277 (2005).
26. W. T. Wang, Z. H. Chen, G. Yang, D. Y. Guan, G. Z. Yang, Y. L. Zhou, and H. B. Lu, "Resonant absorption quenching and enhancement of optical nonlinearity in $\text{Au}:\text{BaTiO}_3$ composite films by adding Fe nanoclusters," *Appl. Phys. Lett.* **83**, 1983–1985 (2003).
27. I. Tanahashi, Y. Manabe, T. Tohda, S. Sasaki, and A. Nakamura, "Optical nonlinearities of Au/SiO_2 composite thin films prepared by a sputtering method," *J. Appl. Phys.* **79**, 1244–1249 (1996).
28. G. W. Milton, *The Theory of Composites* (Cambridge U. Press, 2002).
29. T. B. Jones, *Electromechanics of Particles* (Cambridge U. Press, 1995).
30. S. G. Lu, X. H. Zhu, C. L. Mak, K. H. Wong, H. L. W. Chan, and C. L. Choy, "High tunability in compositionally graded epitaxial barium strontium titanate thin films by pulsed-laser deposition," *Appl. Phys. Lett.* **82**, 2877–2879 (2003).
31. J. D. Jackson, *Classical Electrodynamics* (Wiley, 1975).
32. J. C. Garland and D. B. Tanner, eds., *Electric Transport and Optical Properties of Inhomogeneous Media*, AIP Conference Proceedings No. 40 (American Institute of Physics, 1978).
33. L. Dong, G. Q. Gu, and K. W. Yu, "First-principles approach to dielectric response of graded spherical particles," *Phys. Rev. B* **67**, 224205 (2003).
34. G. Q. Gu and K. W. Yu, "Conductivities of dilute suspensions of graded fibers," *J. Appl. Phys.* **94**, 3376–3383 (2003).
35. J. P. Huang, K. W. Yu, G. Q. Gu, and M. Karttunen, "Electrorotation in graded colloidal suspensions," *Phys. Rev. E* **67**, 051405 (2003).
36. D. Stroud and V. E. Wood, "Decoupling approximation for the nonlinear-optical response of composite media," *J. Opt. Soc. Am. B* **6**, 778–786 (1989).
37. J. C. Maxwell Garnett, "Colours in metal glasses and in metallic films," *Philos. Trans. R. Soc. London, Ser. A* **203**, 385–420 (1904).
38. J. C. Maxwell Garnett, "Colours in metal glasses, in metallic films, and in metallic solutions. II," *Philos. Trans. R. Soc. London, Ser. A* **205**, 237–288 (1906).
39. C. F. Bohren and D. R. Huffman, *Absorption and Scattering of Light by Small Particles* (Wiley, 1983).
40. Z. Hashin and S. Shtrikman, "A variational approach to the theory of the effective magnetic permeability of multiphase materials," *J. Appl. Phys.* **33**, 3125–3131 (1962).
41. K. W. Yu, "Mean field theory for lossy nonlinear composites," *Solid State Commun.* **105**, 689–693 (1998).
42. L. Gao, J. P. Huang, and K. W. Yu, "Effective nonlinear optical properties of composite media of graded spherical particles," *Phys. Rev. B* **69**, 075105 (2004).